lincRNA-Cox2 Functions to Regulate Inflammation in Alveolar Macrophages during Acute Lung Injury

Elektra Kantzari Robinson,* Atesh Worthington,*,† Donna Poscablo,*,† Barbara Shapleigh,* Mays Mohammed Salih,* Haley Halasz,* Lucas Seninge,‡ Benny Mosqueira,* Valeriya Smaliy,* E. Camilla Forsberg,†,‡ and Susan Carpenter*

Our respiratory system is vital to protect us from the surrounding nonsterile environment; therefore, it is critical for a state of homeostasis to be maintained through a balance of inflammatory cues. Recent studies have shown that actively transcribed noncoding regions of the genome are emerging as key regulators of biological processes, including inflammation. *lincRNA-Cox2* is one such example of an inflammatory inducible long intergenic noncoding RNA functioning to fine-tune immune gene expression. Using bulk and single-cell RNA sequencing, in addition to FACS, we find that *lincRNA-Cox2* is most highly expressed in the lung and is most upregulated after LPS-induced lung injury (acute lung injury [ALI]) within alveolar macrophages, where it functions to regulate inflammation. We previously reported that *lincRNA-Cox2* functions to regulate its neighboring protein Ptgs2 in *cis*, and in this study, we use genetic mouse models to confirm its role in regulating gene expression more broadly in *trans* during ALI. Il6, Ccl3, and Ccl5 are dysregulated in the *lincRNA-Cox2*–deficient mice and can be rescued to wild type levels by crossing the deficient mice with our newly generated *lincRNA-Cox2* transgenic mice, confirming that this gene functions in *trans.* Many genes are specifically regulated by *lincRNA-Cox2* within alveolar macrophages originating from the bone marrow because the phenotype can be reversed by transplantation of wild type bone marrow into the *lincRNA-Cox2*–deficient mice. In conclusion, we show that *lincRNA-Cox2* is a *trans*-acting long noncoding RNA that functions to regulate immune responses and maintain homeostasis within the lung at baseline and on LPS-induced ALI. ***The Journal of Immunology*****, 2022, 208: 1886–1900.**

Acute lung injury (ALI) and its more severe form, known as acute respiratory distress syndrome, are caused by dysregulated inflammatory responses resulting from conditions such as sepsis and trauma (1–5). Fundamentally, the characteristics of ALI include neutrophilic alveolitis, dysfunction of barrier properties, microvascular thrombosis, the formation of hyaline membrane, alveolar macrophage (AM) dysfunction, as well as indirect systemic inflammatory responses (6–9). Although a variety of anti-inflammatory pharmacotherapies are available, the morbidity and outcome of ALI/acute respiratory distress syndrome patients remain poor (10–13). Therefore, obtaining a more complete understanding of the molecular mechanisms that drive ALI inflammatory dysfunction is of great importance to improving both the diagnosis and the treatment of the condition.

Long noncoding RNAs (lncRNAs) are a class of noncoding RNAs that include 18,000 in the human and nearly 14,000 in the mouse genome (14, 15). Since their discovery, lncRNAs have been shown to be key regulators of inflammation both in vitro and in vivo (16, 17). Moreover, lncRNAs have also been characterized to be stable and detectable in body fluids (18), and therefore have enormous potential for biomarker discovery in both diagnosis and prognosis applications (19–21). Broadly, lncRNAs have been defined to function in *cis* to regulate their neighboring genes, as well as in *trans* to regulate genes on different chromosomes (16). A number of studies have been conducted to better understand the gene regulatory network between lncRNAs and mRNAs during ALI to identify novel biomarkers (22, 23). In addition to searching for biomarkers for ALI, there have been studies performed to try to understand the functional

*Department of Molecular, Cell and Developmental Biology, University of California Santa Cruz, Santa Cruz, CA; †Institute for the Biology of Stem Cells, University of California-Santa Cruz, Santa Cruz, CA; and ‡Department of Biomolecular Engineering, University of California Santa Cruz, Santa Cruz, CA

ORCIDs: 0000-0003-1427-3897 (E.K.R.); 0000-0003-3676-8735 (A.W.); 0000-0002-6687-3483 (M.M.S.); 0000-0001-6536-6810 (L.S.); 0000-0002-5615-7520 (B.M.); 0000-0002-8740-4299 (E.C.F.); 0000-0002-5600-5404 (S.C.).

Received for publication August 2, 2021. Accepted for publication February 5, 2022.

This work was supported by the California Tobacco-Related Disease Research Program (27IP-0017H to S.C.). This work was supported by California Institute for Regenerative Medicine Facilities Awards CL1-00506 and FA1-00617-1 to the University of California Santa Cruz. E.K.R. was supported by a Foundation for the National Institutes of Health Predoctoral Training Grant (T32 GM008646). This work was also supported by a Howard Hughes Medical Institute Gilliam Fellowship Award, an American Heart Association Predoctoral Fellowship Award (to D.P.), a U.S. Department of Health and Human Services, National Institutes of Health, National Heart, Lung, and Blood Institute F31 Fellowship Award, and a Tobacco-Related Disease Research Program Predoctoral Fellowship Award to A.W.

E.K.R. designed, performed, and analyzed all molecular biology and in vivo experiments for all figures. A.W. and D.P. assisted with flow cytometry and sorting experiments, as well as helped design and perform chimera transplantation experiments. B.S. set up and performed experiments for Fig. 3. M.M.S., H.H., and S.C. assisted with all in vivo experiments. B.M. analyzed bulk RNA sequencing experiments. V.S. helped with analyzing RT-qPCR experiments in Fig. 5. L.S. analyzed all single-cell RNA sequencing datasets. E.C.F. helped with the design and analysis of bone marrow transplantation and chimera experiments. E.K.R. and S.C. conceived and coordinated the project. E.K.R. and S.C. wrote the manuscript with input from all other coauthors.

Address correspondence and reprint requests to Susan Carpenter, Department of Molecular, Cell and Developmental Biology, University of California Santa Cruz, 1156 High Street, Santa Cruz, CA 95064. E-mail address: sucarpen@ucsc.edu

The online version of this article contains supplemental material.

Abbreviations used in this article: ALI, acute lung injury; AM, alveolar macrophage; BAL, bronchiolar lavage fluid; BALF, bronchoalveolar lavage fluid; BM, bone marrow; DC, dendritic cell; GM, granulocyte/myelomonocyte; KO, knockout; lncRNA, long noncoding RNA; Mut, deficient in *lincRNA-Cox2*; MutxTG mice, *lincRNA-Cox2* transgenic mice crossed with the *lincRNA-Cox2* mutant mice; PB, peripheral blood; RNA-seq, RNA sequencing; Tg, transgenic; TG mice, transgenic mice overexpressing *lincRNA-Cox2*; UbC, Ubiquitin C; UCSC, University of California Santa Cruz; WT, wild type.

This article is distributed under The American Association of Immunologists, Inc., Reuse Terms and Conditions for Author Choice articles.

Copyright © 2022 by The American Association of Immunologists, Inc. 0022-1767/22/$37.50

www.jimmunol.org/cgi/doi/10.4049/jimmunol.2100743

mechanisms for lncRNAs during ALI (24). LPS-induced ALI is a commonly used animal model of ALI because it mimics the inflammatory induction and polymorphonuclear cell infiltration observed during clinical ALI (25). One study showed that knocking down MALAT1, a well-studied lncRNA, exerts a protective role in the LPS-induced ALI rat models and inhibited LPS-induced inflammatory response in murine alveolar epithelial cells and murine AMs cells through sponging miR-146a (26). In addition, Xist has been shown to attenuate LPS-induced ALI by functioning as a sponge for miR-146a-5p to mediate STAT3 signaling (27).

Previous work, by ourselves and others, identifies long intergenic noncoding RNA Cox2 (*lincRNA-Cox2*) as a regulator of immune cell signaling in macrophages (28–34). We have previously characterized multiple mouse models to show that *lincRNA-Cox2* functions in vivo to regulate the immune response. We showed that *lincRNA-Cox2* knockout (KO) mice (35) have profound defects in the neighboring protein coding gene Ptgs2. We went on to show that *lincRNA-Cox2* regulates Ptgs2 in *cis* through an enhancer RNA mechanism requiring locus-specific transcription of the lncRNA (Supplemental Fig. 1) (36). To study the function of *lincRNA-Cox2* independently of its role in regulating Ptgs2 in *cis*, we generated a deficient in *lincRNA-Cox2* (Mut) mouse using CRISPR to target the splice sites, resulting in significant loss of the RNA and allowing us to study the role for the RNA in *trans* (Supplemental Fig. 1). We performed an LPS-induced endotoxic shock model and confirmed that *lincRNA-Cox2* is an important positive and negative regulator of immune genes in *trans*. We previously showed that *lincRNA-Cox2* is most highly expressed at steady state in the lung; in this study (Supplemental Fig. 1), we use our mutant model to determine whether *lincRNA-Cox2* can function in *trans* to regulate gene expression in the lung (36). In addition, we characterize a transgenic (Tg) overexpressing mouse model of *lincRNA-Cox2* (Supplemental Fig. 1) and show that the defects in immune gene expression caused by removal of *lincRNA-Cox2* can be rescued by the overexpression of *lincRNA-Cox2* in an LPS-induced ALI model. On a cellular level, we show that *lincRNA-Cox2* is most highly induced after inflammation in AMs, where it functions to regulate signaling. Finally, we show through bone marrow (BM) chimeric studies that *lincRNA-Cox2* expression is coming from BM-derived cells to regulate genes within the lung. Collectively, we show that *lincRNA-Cox2* is a *trans*-acting lncRNA that functions to regulate immune responses and maintain homeostasis within the lung at baseline and on LPS-induced ALI.

Materials and Methods

Mice

Wild type (WT) C57BL/6 mice were purchased from the Jackson Laboratory (Bar Harbor, ME) and bred at the University of California Santa Cruz (UCSC). All mouse strains, including *lincRNA-Cox2* mutant (mice deficient in *lincRNA-Cox2* [Mut]), transgenic mice overexpressing *lincRNA-Cox2* (Tg) and the mutant/transgenic cross (MutxTg) mice, were maintained under specific pathogen-free conditions in the animal facilities of UCSC, and protocols were performed in accordance with the guidelines set forth by UCSC and the Institutional Animal Care and Use Committee.

Generation of lincRNA-Cox2 *Tg and MutxTg mice*

lincRNA-Cox2 Tg mice were generated by using a site-specific integrase-mediated approach described previously (37). In brief, TARGATT mice in the C57/B6 background contain a CAGG promoter within the Hipp11 (H11) locus expressing the full-length *lincRNA-Cox2* (variant 1) as previously cloned (28) generated at the Gladstone (UCSF). These mice were then genotyped using the same TARGATT approach of PCR7/8 (PR432: 5′-GATATCCTTACGGAATACCACTTGCCACCTATCACC-3′, SH176: 5′-TGGAGGAGGACAAACTGGTCAC-3′, SH178: 5′-TTCCCTTTCTGCTTCATCTTGC-3′). The *lincRNA-Cox2* Tg mice were then crossed with the *lincRNA-Cox2* mutant mice and bred to homozygosity to generate the mutant/transgenic mice (MutxTg). For genotyping to assess homozygosity of mutant, we used the primer sets of Mut forward (F): 5′-ATGCCCAGAGACAAAAAGGA-3′ and Mut reverse (R): 5′-GATGGCTGGATTCCTTTGAA-3′, as well as the three-primer set stated earlier.

ALI model

Age- and sex-matched WT, Mut, and *lincRNA-Cox2* MutxTG mice were treated with 3.5 mg/kg LPS using the oropharyngeal intratracheal administration technique. The model of LPS insult via oropharyngeal administration into the lung was previously described in detail (38–40). In brief, mice were sedated using an isoflurane chamber (3% for induction, 1–2% for maintenance), then 60–75 μl of 3.5 mg/kg LPS (from strain O111:B4) or PBS (control) was administered using a pipette intratracheally. Twenty-four hours after LPS treatment, mice were sacrificed using CO_2 and serum, and bronchoalveolar lavage fluid (BALF) and lung were harvested for either cellular assessment by flow cytometry or RNA expression, or sent to Eve Technologies for cytokine/chemokine protein analysis.

LPS shock model

Age- and sex-matched WT, *lincRNA-Cox2* mutant, *lincRNA-Cox2* TG, and *lincRNA-Cox2* MutxTG mice (36) (8–12 wk of age) were injected i.p. with 20 mg/kg LPS (O111:B4). For gene expression analysis and cytokine analysis, mice were euthanized 6 h postinjection. Blood was taken immediately postmortem by cardiac puncture. Statistics were performed using GraphPad Prism.

Transplantation reconstitution assays

Reconstitution assays were performed as previously stated by Poscablo et al. (41), by transplanting double-sorted hematopoietic stem cells (3 million cells per recipient) from Ubiquitin C (Ubc)-GFP^+ whole BM and transplanting into congenic C57BL/6 WT and *lincRNA-Cox2*–deficient mice via retroorbital i.v. transplant generating WT→WT and WT→Mut. Hosts were preconditioned with lethal radiation (~1050 rad) using a Faxitron CP160 x-ray instrument (Precision Instruments).

Harvesting bronchiolar lavage fluid

BALF was harvested as previously stated by Cloonan et al. (42). Forty mice were euthanized by CO_2 narcosis, the tracheas cannulated, and the lungs lavaged with 0.5-ml increments of ice-cold PBS eight times (4 ml total); samples were combined in 50-ml conical tubes. BALF was centrifuged at 500 × *g* for 5 min. A total of 1 ml RBC lysis buffer (Sigma-Aldrich) was added to the cell pellet and left on ice for 5 min followed by centrifugation at 500 × *g* for 5 min. The cell pellet was resuspended in 500 μl PBS, and leukocytes were counted using a hemocytometer. Specifically, 10 μl was removed for cell counting (performed in triplicate) using a hemocytometer. Cells were plated in sterile 12-well plates at 5e5/well (total of 8 wells) and used complete DMEM with 25 ng/ml GM-CSF harvested from our recently generated cell line that produces GM-CSF termed supernatant GM-CSF or supCM-CSF (43).

Lung tissue harvesting for cytokine measurement

Mice were humanely sacrificed, and their lungs were excised. The whole lungs were snap frozen and homogenized, and the resulting homogenates were incubated on ice for 30 min and then centrifuged at 300 × *g* for 20 min. The supernatants were harvested, passed through a 0.45-μm pore size filter, and used immediately or stored at −70°C, then sent to Eve Technologies for measurements of cytokines/chemokines.

Cell culture of primary AMs

BALF isolation was performed on 10 WT and 10 *lincRNA-Cox2* mutant mice; then cells were pooled, counted, and plated. At 24 h post-BALF isolation, medium was removed, and fresh complete DMEM with 25 ng/ml supGM-CSF was added (43). All cells that adhere to the surface of the plate are considered AMs as previously determined by Chen et al. (44). After new medium was added, AMs were stimulated with 200 ng/ml LPS (L2630-10MG; Sigma). Harvest of supernatant was 6 h poststimulation. Harvested supernatant was sent to Eve Technologies for cytokine analysis. The experiment was performed twice, using a total of 40 mice. Statistics were performed using GraphPad Prism.

RNA isolation, cDNA synthesis, and real-time quantitative PCR

Total RNA was purified from cells or tissues using Direct-zol RNA MiniPrep Kit (R2072; Zymo Research) and TRIzol reagent (T9424; Ambion) according to the manufacturer's instructions. RNA was quantified and assessed for purity using a NanoDrop spectrometer (Thermo Fisher). Equal amounts of RNA (500–1000 ng) were reverse transcribed using iScript Reverse Transcription Supermix (1708841; Bio-Rad), followed by qPCR using iQ SYBR Green Supermix reagent (1725122; Bio-Rad) with the

following parameters: 50°C for 2 min and 95°C for 2 min, followed by 40 cycles of 95°C for 15 s, 60°C for 30 s, and 72°C for 45 s, followed by melt-curve analysis to control for nonspecific PCR amplifications. Oligos used in qPCR analysis were designed using Primer3 Input version 0.4.0 (https://bioinfo.ut.ee/primer3-0.4.0/).

Gene expression levels were normalized to Gapdh or Hprt as housekeeping genes. Primers used were: Gapdh F, 5′-CCAATGTGTCCGTCGTGGATC-3′; Gapdh R, 5′-GTTGAAGTCGCAGGAGACAAC-3′; Hprt F, 5′-TGCTCGAGATGTCATGAAGG-3′; Hprt R, 5′-ATGTCCCCCGTTGACTGAT-3′; lincRNACox2 F, 5′-AAGGAAGCTTGGCGTTGTGA-3′; and lincRNACox2 R, 5′-GAGAGGTGAGGAGTCTTATG-3′.

ELISA

The concentration of Il6 and Ccl5 levels in the serum and BAL of WT, Mut, *lincRNA-Cox*2 Tg, and *lincRNA-Cox2* MutxTg mice were determined using the DuoSet ELISA kits (DY1829 and DY478; R&D) according to the manufacturer's instructions.

Lung tissue harvesting for cellular analysis

Mice were humanely sacrificed, and their lungs were excised. Lung was inflated with a digestion solution containing 1.5 mg/ml Collagenase A (Roche) and 0.4 mg/ml DNaseI (Roche) in HBSS plus 5% FBS and 10 mM HEPES. Trachea was tied off with 2.0 sutures. The heart and mediastinal tissues were carefully removed, and the lung parenchyma was placed in 5 ml of digestion solution and incubated at 37°C for 30 min with gentle vortexing every 8–10 min. On completion of digestion, 25 ml of PBS was added, and the samples were vortexed at maximal speed for 30 s. The resulting cell suspensions were strained through a 70-μm cell strainer and treated with ACK RBC lysis solution. Then the cells were stained using the previously published immune (45) and epithelial (46) cellular panels.

Flow cytometry analysis and sorting

After cells were isolated and counted, ~2×10^6 cells per sample were incubated in blocking solution containing 5% normal mouse serum, 5% normal rat serum, and 1% FcBlock (eBioscience) in PBS and then stained with a standard panel of immunophenotyping Abs (see Supplemental Table II for a list of Abs, clones, fluorochromes, and manufacturers) for 30 min at room temperature (45). Data were acquired, and compensation was performed on the BD Aria II and Attune NxT (Thermo Fisher) flow cytometer at the beginning of each experiment. Data were analyzed using FlowJo v10. Cell sorting was performed on a BD Aria II. The collected cells were harvested for RNA, and RT-qPCR was performed to measure *lincRNA-Cox2*. Analysis was performed using FlowJo analysis software (BD Biosciences).

RNA sequencing analysis

Generation of the RNA sequencing (RNA-seq) data (accession numbers GSE117379 [https://www.ncbi.nlm.nih.gov/gds/?term=GSE117379] and GSE94749 [https://www.ncbi.nlm.nih.gov/gds/?term=GSE94749]) and analysis of differential gene expression have been described previously (36, 47). RNA-seq 50- or 30-bp reads, respectively, were aligned to the mouse genome (assembly GRCm38/mm10) using TopHat. The Gencode M13 gtf was used as the input annotation. Differential gene expression specific analyses were conducted with the DESeq2 R package. Specifically, DESeq2 was used to normalize gene counts, calculate fold change in gene expression, estimate p values and adjusted p values for change in gene expression values, and perform a variance stabilized transformation on read counts to make them amenable to plotting.

Single-cell RNA-seq analysis

Generation of the single-cell RNA sequencing data (Gene Expression Omnibus accession numbers GSE120000 [https://www.ncbi.nlm.nih.gov/gds/?term=GSE120000] and GSE113049 [https://www.ncbi.nlm.nih.gov/gds/?term=GSE113049]) and analysis of gene expression have been described previously (48, 49). All analysis was performed using the Scanpy package (50). Unless specified, default parameters were used.

For GSM3391587 (https://www.ncbi.nlm.nih.gov/gds/?term=GSM3391587), count matrix was processed according to the original study. In brief, the count matrix was normalized to log(10K+1) transcripts, and highly variable genes were selected with the following parameters: minimum dispersion = 0.2, minimum mean = 0.15. Those genes were used to compute principal components, out of which the top 6 were selected for clustering and visualization. The t-distributed stochastic neighbor embedding coordinates were computed using the top six principal components, and Louvain clustering was performed based on the k-nearest neighbor graph (k = 30) derived from the principal components.

For GSE113049 (https://www.ncbi.nlm.nih.gov/gds/?term=GSE113049), the count matrix was processed as follows: cells with <200 detected genes were removed, and genes detected in <3 cells were removed. Cells with >5% of mitochondrial content were further excluded from the analysis. Counts were normalized to log(10K+1) transcripts. The t-distributed stochastic neighbor embedding coordinates and cell-type labels were obtained from public files made available by the authors of the original study.

Results

Immune gene expression is altered in the lungs of lincRNA-Cox2*–deficient mice*

To determine the role for *lincRNA-Cox2* in the lung, we first examined RNA-seq data of WT versus Mut mice treated with PBS to compare gene expression profiles (36) (Fig. 1A). We found 85 genes downregulated and 41 genes upregulated in the Mut lungs compared with WT (Fig. 1B, Supplemental Table I). Gene Ontology analysis showed that both the downregulated and upregulated genes were associated with the immune system, metabolism, and response to stimulus (Fig. 1C, 1D), which are similar to pathways that *lincRNA-Cox2* has previously been associated with in BM-derived macrophages (28). To determine whether loss of *lincRNA-Cox2* impacts protein expression, we performed ELISAs on lung homogenates from WT and *lincRNA-Cox2*–deficient (Mut) mice (Fig. 1E). Although many genes remained unchanged at baseline (PBS) between the WT and *lincRNA-Cox2* Mut lungs (Supplemental Fig. 2A–H), we did find that Il-12p40, Cxcl10, Ccl3, Ccl4, Cxcl2, Ccl5, and Ccl19 are all significantly upregulated in the Mut lungs (Fig. 1F–L). Interestingly, none of these cytokines are upregulated at the RNA level in our whole-lung tissue RNA-seq, suggesting that they might be regulated posttranscriptionally or that they are regulated in only a small subset of cells that cannot be easily captured from the whole-lung lysate RNA-seq data (Supplemental Fig. 2I–P).

Finally, we measured the immune cell repertoire in the bronchiolar lavage fluid (BAL) of WT and *lincRNA-Cox2*–deficient (Mut) mice and found that B cells and dendritic cells (DCs), although at very low expression levels in both strains, are significantly lower at baseline in the mutant mice (Fig. 1M). These findings indicate that *lincRNA-Cox2* functions as both a positive and a negative regulator of immune gene expression that can impact the cellular milieu within the lung at steady state in mice.

lincRNA-Cox2 *regulates the proinflammatory response during ALI*

Our data suggest that *lincRNA-Cox2* plays a role in regulating immune gene expression at steady state; therefore, we wanted to determine whether loss of *lincRNA-Cox2* could impact the immune response during ALI. We used a 24-h LPS-induced ALI model, because *lincRNA-Cox2* is highly expressed at this time point (Fig. 2A, 2B). We assessed the immune cell repertoire within the BAL by flow cytometry in WT and *lincRNA-Cox2* mutant mice after LPS challenge and found that the most abundant and critical cell type, neutrophils, was significantly reduced when *lincRNA-Cox2* was removed (Fig. 2C). We also assessed the cytokine and chemokine response both in the BAL and in the serum of WT and *lincRNA-Cox2* Mut mice by ELISA. We found that Il6, Ccl3, and Ccl4 were downregulated in the serum and BAL of *lincRNA-Cox2* Mut mice (Fig. 2D–F). In addition, several proteins were specifically affected either in the serum or BAL, such as Ccl5 and Ccl22, which were upregulated in the serum (Fig. 2G, 2H), while Ifnb1 was upregulated only in the BAL of the Mut mice (Fig. 2I). Consistent with our previous work, Tnfa remains unchanged between WT and *lincRNA-Cox2* Mut mice (Fig. 2J). These data suggest that *lincRNA-Cox2* exerts different effects within the lung compared with the periphery, and that *lincRNA-Cox2* can impact acute inflammation at the protein and cellular levels within the lung.

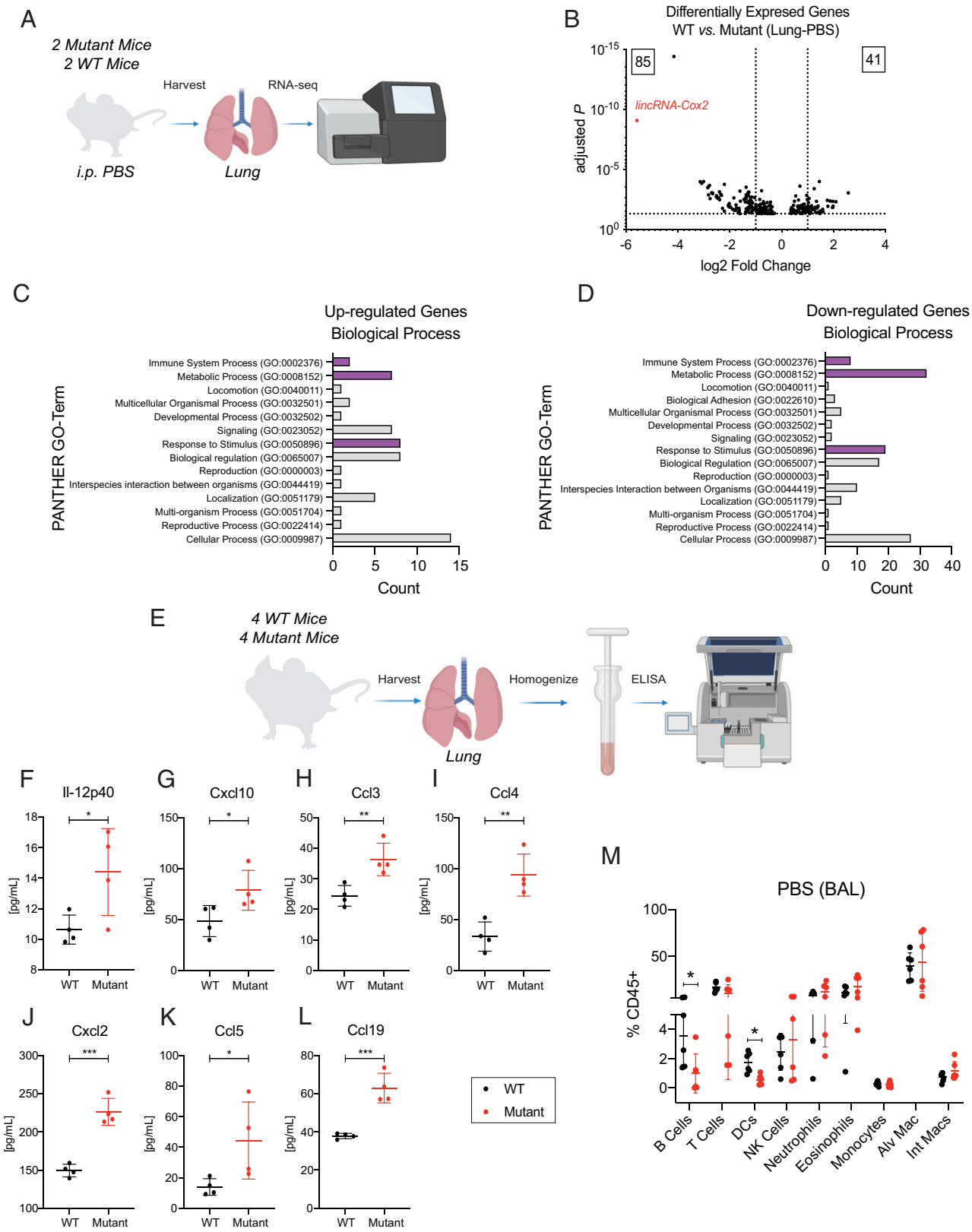

FIGURE 1. *lincRNA-Cox2* regulates immune signaling within the lung during homeostasis. (**A**) Schematic of RNA-seq analysis of WT and Mut lungs at baseline. (**B**) Volcano plot of differentially expressed genes from WT versus Mut lungs. Biological process Gene Ontology of (**C**) upregulated genes and (**D**) downregulated genes. (**E**) Schematic of cytokine analysis of lung homogenates from WT and Mut mice. Multiplex cytokine analysis was performed on lung homogenates for (**F**) Il-12p40, (**G**) Cxcl10, (**H**) Ccl3, (**I**) Ccl4, (**J**) Cxcl2, (**K**) Ccl5, and (**L**) Ccl19. (**M**) Flow cytometry analysis of immune cells in the BAL at baseline gated on $CD45^+$ cells. The Student *t* test used to determine the significance between WT and mutant mice. Asterisks indicate statistical significance (*$p > 0.05$, **$p \geq 0.01$, ***$p > 0.005$).

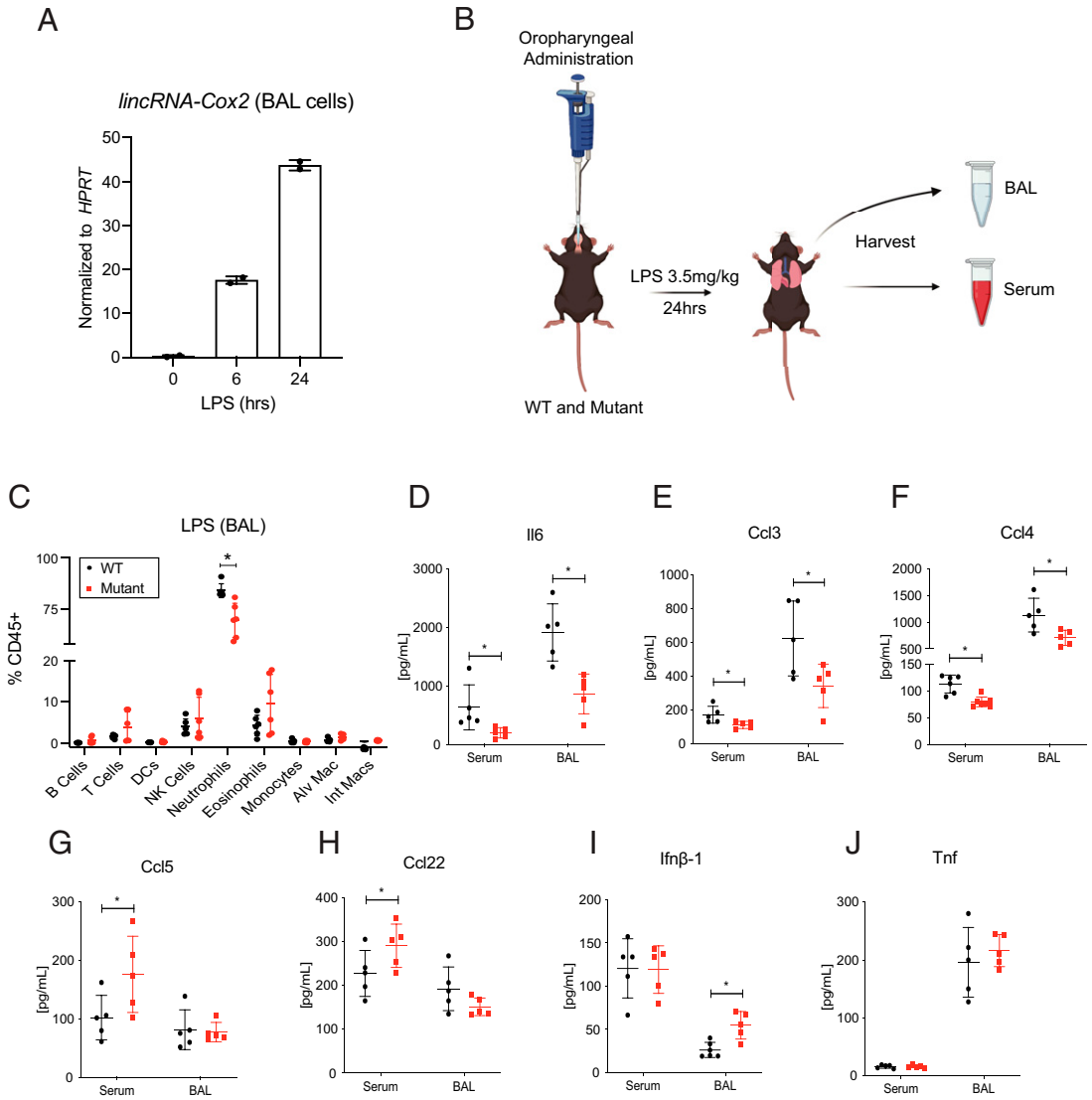

FIGURE 2. *lincRNA-Cox2* positively regulates the proinflammatory response during ALI. (**A**) Six WT mice were treated with either PBS or 3.5 mg/kg LPS via the oropharyngeal route. After 6 and 24 h, BALs were harvested, and RNA was isolated. *lincRNA-Cox2* was measured by RT-qPCR in pooled BAL cells. (**B**) ALI schematic depicting the oropharyngeal route of 3.5 mg/kg LPS administration in WT and mutant. Mice were sacrificed after 24 h, followed by harvesting serum and BAL. (**C**) BAL cells were analyzed by flow cytometry to assess recruitment of immune cells in WT and immune cells gated off $CD45^{+}$. Multiplex cytokine analysis was performed on serum and BAL for (**D**) Il6, (**E**) Ccl5, (**F**) Ccl3, (**G**) Ccl4, (**H**) Ccl22, (**I**) Ifnb-1, and (**J**) Tnf. The Student *t* test used to determine the significance between WT and mutant mice. Asterisks indicate statistical significance (*$p > 0.05$).

Generation and characterization of a Tg mouse model overexpressing lincRNA-Cox2

We have determined that *lincRNA-Cox2* is critical in regulating inflammation at baseline during a septic shock model (36) and in this study during an ALI model. To confirm that *lincRNA-Cox2* is functioning in *trans*, we generated a Tg *lincRNA-Cox2* mouse line using the TARGATT system, which allows for stable integration of *lincRNA-Cox2* into the H11 locus (37) (Fig. 3A). The inserted cassette is carrying a CAG promoter, *lincRNA-Cox2*, and an SV40 polyA stop cassette. Mice were bred to homozygosity (Supplemental Fig. 3A–D), and *lincRNA-Cox2* levels were measured in WT and Tg BM-derived macrophages (Fig. 3B). As expected, *lincRNA-Cox2* is highly expressed in the Tg macrophages with no difference in expression after LPS stimulation (Fig. 3B).

Next, we performed a septic shock model of WT and Tg mice to determine whether overexpression of *lincRNA-Cox2* can impact the immune response (Fig. 3C). As expected, *lincRNA-Cox2* is highly expressed in the lung tissue of the Tg mice and, interestingly, we observe increased levels of Il6, while other *lincRNA-Cox2* target genes, such as Ccl5, are not affected. This suggests that overexpression of *lincRNA-Cox2* can have the opposite phenotype to knocking out the gene to regulate Il6 within the lung (Fig. 3D, Supplemental Fig. 3E–G). We harvested serum from the mice and found higher levels of Csf1 and lower levels of Il10 (Fig. 3E, 3F) in the mice overexpressing *lincRNA-Cox2*. Other inflammatory cytokines, including Il6, Ccl5, Ccl3, and Ccl4, were unaltered in *lincRNA-Cox2* Tg mouse serum (Fig. 3G–J, Supplemental Fig. 3H–K). These data suggest that overexpression of *lincRNA-Cox2* does not have broad impacts on gene expression during acute systemic inflammation.

Next, we assessed whether overexpression of *lincRNA-Cox2* dysregulated the inflammatory responses within the lung by using the LPS-induced ALI model (Fig. 4A). First, we performed RT-qPCR and confirmed that the overexpression of *lincRNA-Cox2* did not alter the expression of Ptgs2 in the BAL, consistent with our previous findings that it is regulated in *cis* and not in *trans* (Fig. 4B, 4C)

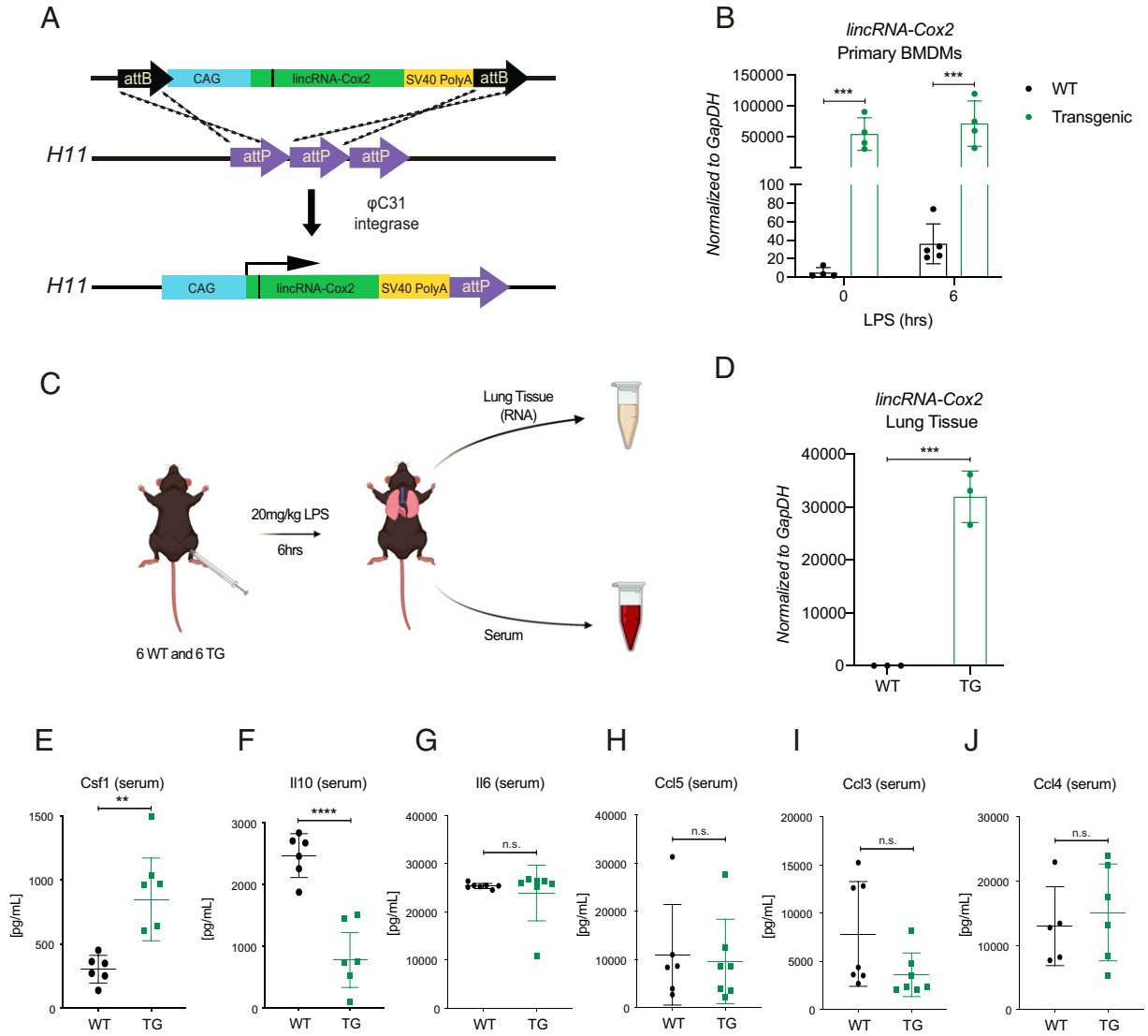

FIGURE 3. Characterization of *lincRNA-Cox2* Tg mouse. (**A**) We have generated a Tg *lincRNA-Cox2* mouse line using the TARGATT system. This approach allows for stable integration of *lincRNA-Cox2* into the H11 locus. Our inserted cassette is carrying a CAG promoter, *lincRNA-Cox2*, and an SV40 polyA stop cassette. (**B**) *lincRNA-Cox2* levels measured in WT and Tg BM-derived macrophages with and without LPS for 6 h, normalized to GAPDH. (**C**) Schematic of 20 mg/kg LPS septic shock model of WT and Tg mice. (**D**) lincRNA-Cox2 measured by RT-qPCR in lung tissue. Serum was harvested and ELISAs were performed to measure (**E**) Csf1, (**F**) Il10, (**G**) Il6, (**H**) Ccl5, (**I**) Ccl3, and (**J**) Ccl4. The Student *t* test was used to determine the significance between WT and TG mice. Asterisks indicate statistical significance (**$p \geq 0.01$, ***$p > 0.005$, ****$p > 0.001$).

(36). To assess the function of *lincRNA-Cox2* in the lung, we then measured the immune cell repertoire within the BAL by flow cytometry in WT and *lincRNA-Cox2* TG mice after LPS challenge and found no significant difference in cell numbers (Fig. 4D). Finally, using both BAL and serum, we measured the cytokine and chemokine profiles of WT and *lincRNA-Cox2* TG mice by ELISA. Interestingly, we found that overexpression of *lincRNA-Cox2* resulted in an upregulation of Il6 and Ccl3 (Fig. 4E, 4F) in the BAL after ALI, which is the opposite phenotype to the deficient mice (Fig. 2). Ccl4 levels trend upward but do not reach significance (Fig. 4G). The *lincRNA-Cox2* Tg mice also showed a specific downregulation in Timp1 in the BAL during ALI (Fig. 4H) and an upregulation of Il10 (Fig. 4I) in the serum. Consistent with knocking down *lincRNA-Cox2*, overexpressing this gene did not alter the regulation of Tnf in either the BAL or the serum (Fig. 4J). These data suggest that *lincRNA-Cox2* functions in *trans* to regulate immune genes during acute inflammation.

lincRNA-Cox2 *functions in trans to regulate acute inflammation*

To confirm that *lincRNA-Cox2* is regulating genes in *trans* after in vivo challenge with LPS, we crossed the Mut mice with the Tg mice overexpressing *lincRNA-Cox2* (TG), generating mice labeled throughout as MutxTG (Fig. 5A, Supplemental Fig. 4A, 4B). We first performed an i.p. endotoxic shock model to determine whether we could rescue the *lincRNA-Cox2* phenotype identified in our previous study (36) (Fig. 5B). As expected, *lincRNA-Cox2* expression is significantly reduced in the lung tissue and BAL of the deficient (Mut) mice and highly expressed in the MutxTG mouse (Fig. 5C, 5D). We found that Ccl5 and Cxcl10 are expressed at higher levels in the BAL and serum of *lincRNA-Cox2* mutant mice (Fig. 5E–H), and the expression levels can be rescued by *trans* expression of *lincRNA-Cox2* in the MutxTG mice returning to WT levels.

Next, we wanted to determine whether Tg overexpression of *lincRNA-Cox2* can reverse the phenotype observed in the deficient

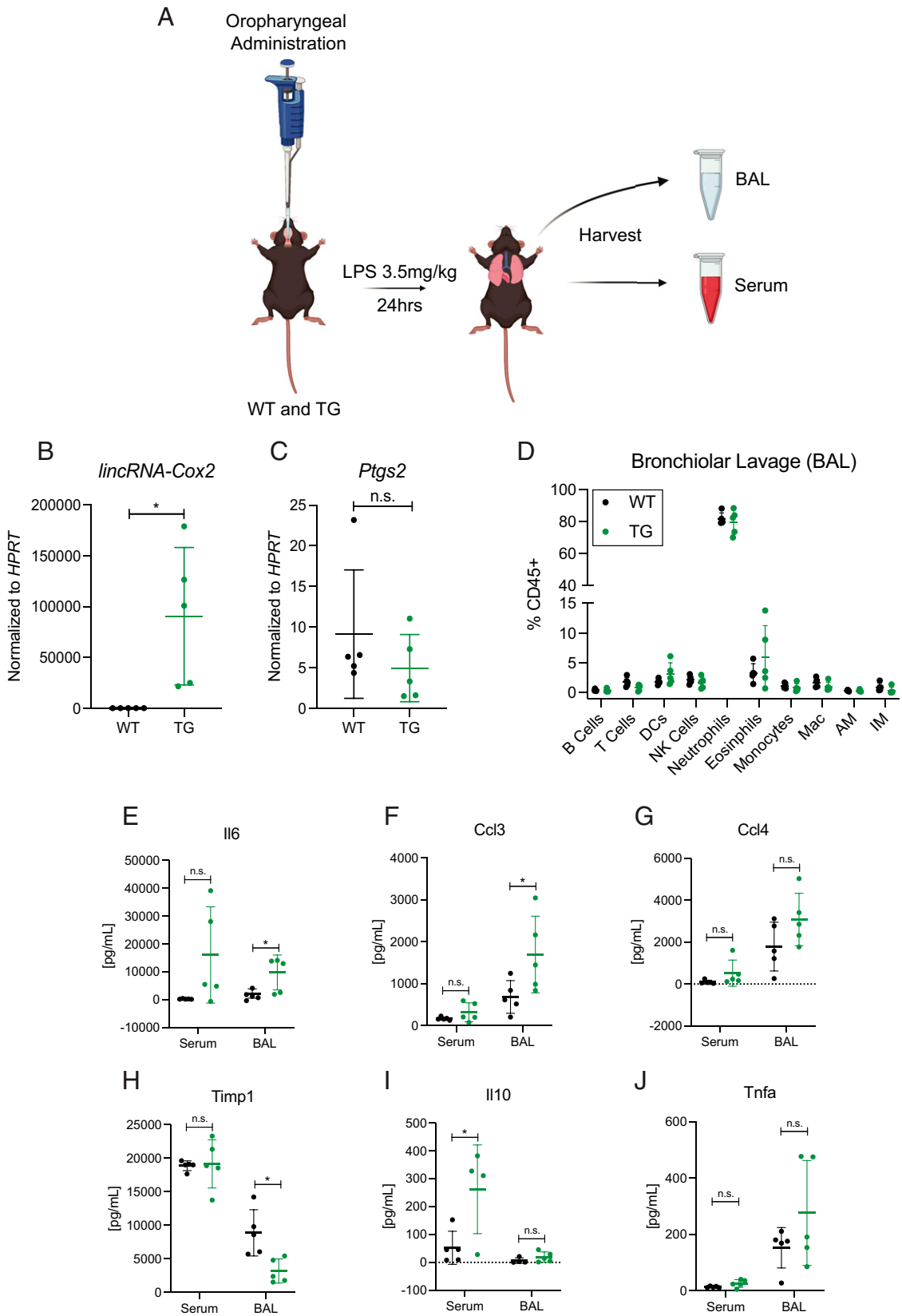

FIGURE 4. Overexpression of *lincRNA-Cox2* heightens inflammation during ALI. (**A**) ALI schematic depicting the oropharyngeal route of 3.5 mg/kg LPS administration in WT and TG. Mice were sacrificed after 24 h, followed by harvesting serum and BAL. (**B** and **C**) *lincRNA-Cox2* (B) and Ptgs2 (C) measured by RT-qPCR in BAL cells. (**D**) BAL cells were analyzed by flow cytometry to assess recruitment of immune cells in WT and immune cells gated off $CD45^{+}$. Multiplex cytokine analysis was performed on serum and BAL for (**E**) Il6, (**F**) Ccl3, (**G**) Ccl4, (**H**) Timp1, (**I**) Il10, and (**J**) Tnfa. Student *t* test was used to determine significance, and asterisks indicate statistical significance (*$p > 0.05$).

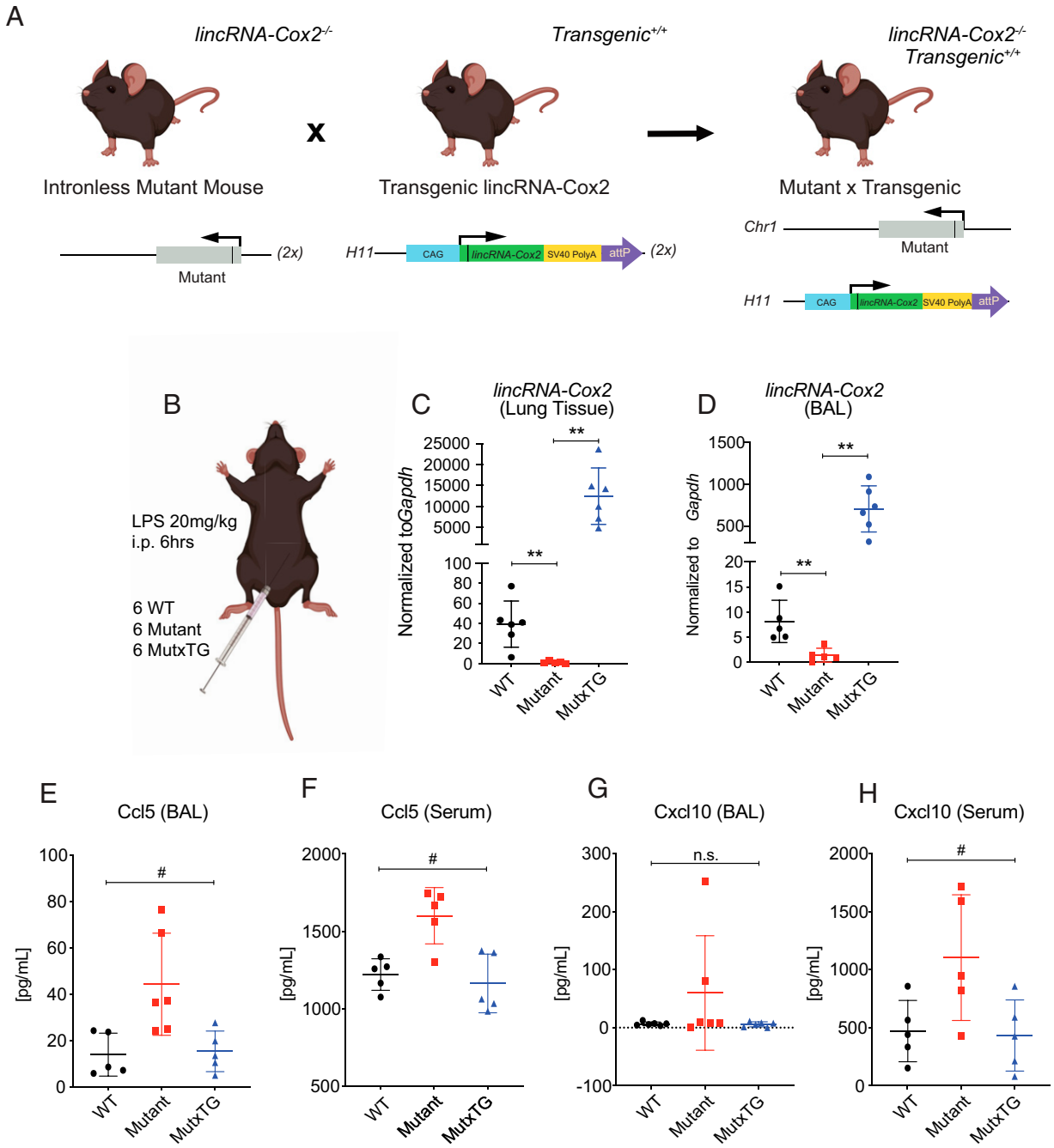

FIGURE 5. *lincRNA-Cox2* functions in *trans* to regulate the innate immune system in a septic shock model. (**A**) Schematic depicting i.p. route of LPS infection in WT, Mut, and MutxTg mice. (**B**) WT, Mut, and TgxMut mice were challenged with 20 mg/kg LPS, and body temperatures were measured. Mice were sacrificed after 6 h; then BAL, lungs, and cardiac punctures were performed. BAL and lungs were harvested for gene expression analysis by RT-qPCR for *lincRNA-Cox2* (**C** and **D**) and Ccl5 (**E** and **F**). BAL and isolated serum were sent for multiplex cytokine analysis (**G** and **H**). Each dot represents an individual animal. Student *t* tests were performed using GraphPad Prism7. Asterisks indicate statistically significant differences between mouse lines (**$p > 0.01$). One-way ANOVA was used to determine significance between WT, Mut, and MutxTG mice ($^{\#}p > 0.05$).

mice during ALI (Fig. 6A). We assessed immune cell recruitment in both the BAL and lung tissue by flow cytometry in WT, Mut, and MutxTG mice. Again, we found that neutrophils are the only immune cell that was significantly lower in *lincRNA-Cox2* mutant mice, while neutrophil recruitment in MutxTG mice was rescued and returned to WT levels (Fig. 6B, 6C). Next, we performed ELISAs on harvested lung tissue, BAL, and serum to measure the protein concentration of cytokines and chemokines. We found that Il6, Ccl5, Ccl3, Ccl4, Ccl22, and Ifnb1 are consistently significantly dysregulated in the *lincRNA-Cox2* mutant mice, and again this phenotype could be rescued back to WT levels by the Tg overexpression of *lincRNA-Cox2* (MutxTG) (Fig. 6D–I). Interestingly, Il6, Ccl3, Ccl4, and Ifnb1 are all significantly different in the BAL, while Ccl5 and Ccl22 are significantly dysregulated only in the lung tissue, suggesting that *lincRNA-Cox2* can impact proteins in a cell-specific manner. These cytokines are not significantly altered at the transcript level (Supplemental Fig. 4C–E). We found that Tnf is consistently unaltered between all genotypes (Fig. 6J). From these data we conclude that *lincRNA-Cox2* functions in *trans* to regulate the lung immune response during acute inflammation.

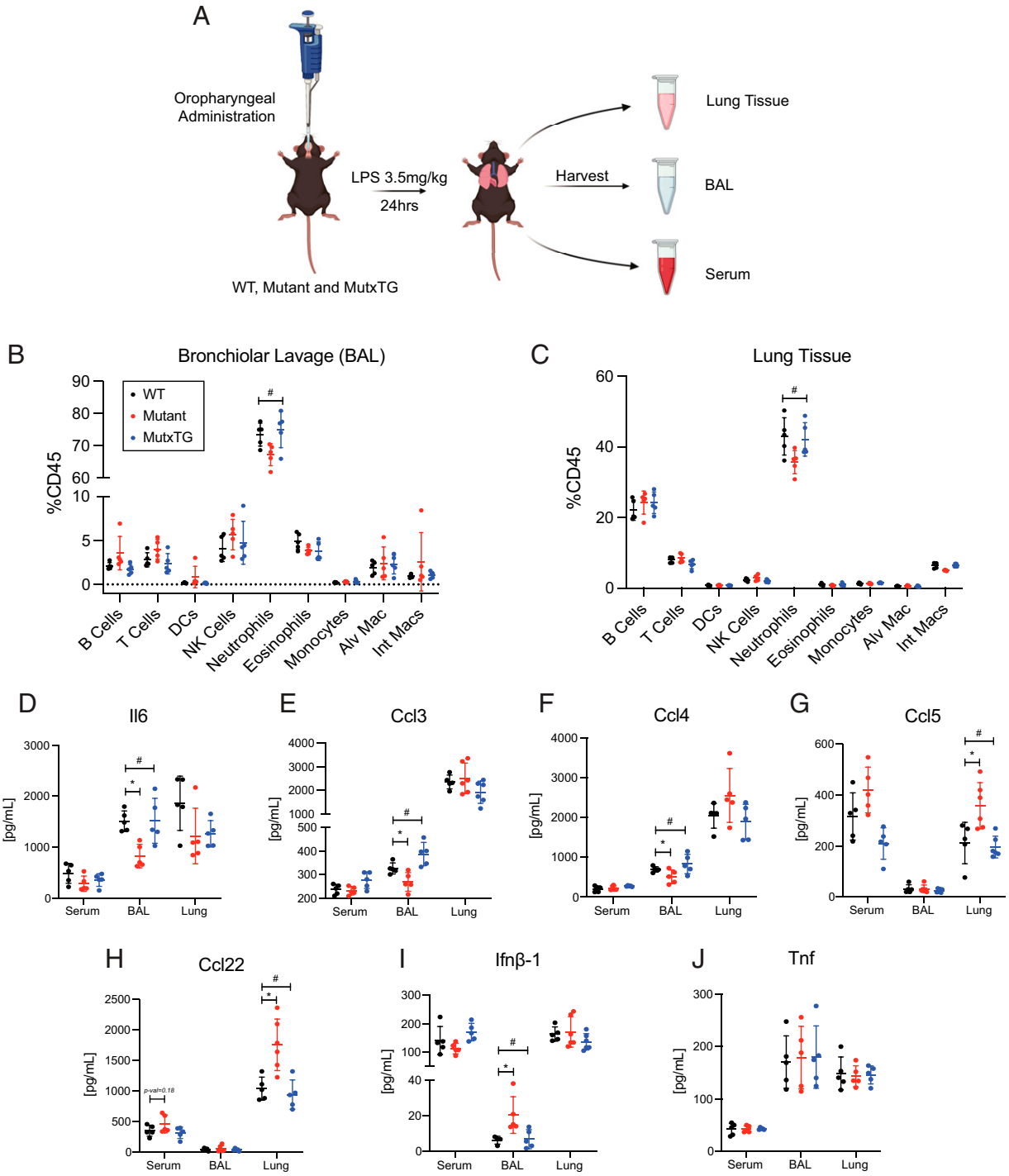

FIGURE 6. *lincRNA-Cox2* regulates the proinflammatory response in the lung in *trans*. (**A**) Generation of *lincRNA-Cox2* MutxTG homozygous mouse. (**B**) ALI schematic depicting the oropharyngeal route of 3.5 mg/kg LPS administration in WT, Mut, and MutxTG. Mice were sacrificed after 24 h, followed by harvesting lung tissue, serum, and BAL. (**C** and **D**) BAL (C) and lung (D) cells were analyzed by flow cytometry to assess recruitment of immune cells in WT and immune cells gated off $CD45^{+}$. Multiplex cytokine analysis was performed on serum, BAL, and lung tissue for (D) Il6, (**E**) Ccl3, (**F**) Ccl4, (**G**) Ccl5, (**H**), Ccl22, (**I**) Ifnb1, (**J**) Tnf. Student *t* test was used to determine significance between WT and Mut mice ($^{*}p > 0.05$). One-way ANOVA was used to determine significance between WT, Mut, and MutxTG mice ($^{\#}p > 0.05$).

lincRNA-Cox2 *positively and negatively regulates immune genes in primary AMs*

To understand how *lincRNA-Cox2* could be regulating acute inflammation, we first wanted to determine in which cell types *lincRNA-Cox2* is most highly expressed within the lung. First, we used publicly available single-cell RNA sequencing (scRNA-seq) data from two LPS-induced lung injury studies (48, 49). Overall, *lincRNA-Cox2* expression was very low in these datasets (Supplemental Fig. 5A–E). There was a slight increase in expression in all alveolar epithelial type II cellular populations (Supplemental Fig. 5D, 5E). Due to the expression level limitations of publicly available scRNA-seq datasets, we next performed FACS to isolate all cell types of interest in the lung at baseline and after LPS-induced lung injury (36). Using RT-qPCR, we found that *lincRNA-Cox2* was most highly expressed in neutrophils at

both baseline and after LPS stimulation when normalized to cell count (Supplemental Fig. 5F, 5G). Interestingly, AMs were identified as the cell type with the highest induction of *lincRNA-Cox2* after LPS stimulation (Fig. 7A).

Because *lincRNA-Cox2* is most highly induced in AMs, we wanted to determine whether this was the cell type contributing to the cytokine and chemokine changes in Mut mice after inflammatory challenge. To do this, we harvested BAL from WT and *lincRNA-Cox2* mutant mice to culture primary AMs and treated them with LPS for 24 h (Fig. 7B). First, *lincRNA-Cox2* induction was validated using RT-qPCR with in vitro LPS-stimulated WT AMs, while expression as expected is diminished in the *lincRNA-Cox2*–deficient AMs (Fig. 7B, 7C). Finally, we assessed the level of cytokine and chemokine expression from primary AMs by ELISA. We confirmed significant dysregulation of Il6, Ccl5, Ccl3, Ccl4, and Ccl22 in primary AMs, which are consistent with the in vivo data (Fig. 7D–L). Performing RT-qPCR on primary AMs, we found that these cytokines are not significantly dysregulated at the level of transcription (Supplemental Fig. 5H–K). In addition, we found novel dysregulation of Cxcl2, Cxcl1, and Cxcl10 specific to AMs from the *lincRNA-Cox2*–deficient mice not detected in our ALI model. Tnf remains consistently unchanged between WT and Mut in AMs and in vivo studies (Fig. 7M). These data indicate that mechanistically *lincRNA-Cox2* is functioning to regulate protein expression primarily within primary AMs.

Peripheral immune cells drive the regulatory role of lincRNA-Cox2 *during ALI*

From our in vivo mouse models, we can conclude that *lincRNA-Cox2* functions in *trans* to regulate immune genes and cellular milieu within the lung during ALI. Using previously generated data of sorted resident and recruited AMs from mice exposed to LPS-induced ALI (Supplemental Fig. 6A) from Mould et al. (47), we found that *lincRNA-Cox2* is expressed in both cell types. When comparing the AM subsets, we found that *lincRNA-Cox2* was more highly expressed in recruited AMs at day 3 of ALI (Supplemental Fig. 6B).

To determine whether *lincRNA-Cox2* functions through BM-derived immune cells, we performed BM transplantation experiments using Ubc-GFP WT BM to enable us to easily track chimerism through measurement of GFP. Ubc-GFP WT BM was transplanted into *lincRNA-Cox2* mutant mice and WT mice generating WT→WT and WT→Mut mice (Fig. 8A). First, we determined the reconstitution of hematopoietic stem cells by measuring donor chimerism (GFP%) in the peripheral blood (PB) for the duration of the 8 wk. We found that both the WT→WT and WT→Mut mice have 100% donor reconstitution of granulocytes/myelomonocytes (GMs) and B cells and ~75% donor T cells in PB (Fig. 8B–D). Although there was a small but significant decrease in T cell reconstitution in WT→Mut mice, we found there was no significant reconstitution difference of GMs or B cells between WT→WT and WT→Mut mice.

After 8 wk when the immune system was fully reconstituted, we performed the LPS ALI model on the chimera WT→WT and WT→Mut mice. We found that the percentage of donor reconstitution within PB was 100%, indicating a successful BM transplantation (Fig. 8B–D, Supplemental Fig. 6C–K) (51). We found that the decrease in neutrophil recruitment that we identified in the *lincRNA-Cox2* mutant mice (Figs. 2B, 6B, 6C, 7E, Supplemental Fig. 6L) was rescued in the WT→Mut model back to similar levels to the WT→WT mice (Fig. 8E). Furthermore, the altered expressions of Il6, Ccl3, and Ccl4 found in the *lincRNA-Cox2* mutant mice were also returned to WT levels in the WT→Mut mice (Figs. 2C–E, 6D–F, 8F–H). As expected, Tnf acts as a control cytokine showing no difference across genotypes (Fig. 8I). These data suggest that *lincRNA-Cox2* is functioning through an immune cell from the BM, most likely AMs, to regulate acute inflammatory responses within the lung.

Discussion

lncRNAs are rapidly emerging as critical regulators of biological responses, and in recent years there have been several studies showing that these genes play key roles in regulating the immune system (16). However, very few studies have functionally characterized lncRNAs using mouse models in vivo. We and others have studied the role for *lincRNA-Cox2* in the context of macrophages and shown that it can act as both a positive and a negative regulator of immune genes (28–34). We previously characterized two mouse models of *lincRNA-Cox2*, a KO and an intronless splicing Mut. We identified *lincRNA-Cox2* as a *cis*-acting regulator of its neighboring protein coding gene Ptgs2 using the KO mouse model. To study the role for *lincRNA-Cox2* independent of its *cis* role regulating Ptgs2, we generated the splicing Mut mouse model (Supplemental Fig. 1). This model enabled us to show that knocking down *lincRNA-Cox2* impacts a number of immune genes, including Il6 and Ccl5, in an LPS-induced endotoxic shock model (36). In this study, we make use of the mutant mouse model to study the role for *lincRNA-Cox2* in regulating immune responses in the lung, where *lincRNA-Cox2* is most highly expressed, both at steady state and after LPS-induced ALI. Both neutrophil recruitment and chemokine/cytokine induction are hallmarks of ALI (38, 52, 53), and in this study, we provide in vivo and in vitro evidence that *lincRNA-Cox2* plays an important role in these processes.

We found that loss of *lincRNA-Cox2* at baseline resulted in the upregulation and downregulation of a number of genes that regulate the immune system and metabolism (Fig. 1A–D), indicating that *lincRNA-Cox2* is a key transcriptional regulator of gene expression within lung tissue. In addition, we measured immune cells and found that at baseline DCs and B cells were lower in the *lincRNA-Cox2* mutant mice. Lung DCs serve as functional signaling/sensing units to maintain lung homeostasis by orchestrating host responses to benign and harmful foreign substances, while B cells are crucial for Ab production, Ag presentation, and cytokine secretion (23, 54). Having fewer DCs and B cells at steady state could lead to an increased risk for inflammatory diseases (55, 56). This indicates that *lincRNA-Cox2* plays an important role in maintaining lung homeostasis because gene expression and cellular abundance are altered by the loss of *lincRNA-Cox2*.

Although we identify *lincRNA-Cox2* as a crucial element for maintaining lung homeostasis, we next performed LPS-induced ALI to assess the importance of *lincRNA-Cox2* during active inflammation. Using a 24-h time point, which shows the maximum influx of polymorphonuclear cells and cytokine/chemokine expression and the highest expression of *lincRNA-Cox2* (Fig. 2A) (52), we found that loss of *lincRNA-Cox2* led to a decrease in neutrophil recruitment and altered cytokine/chemokine expression in both the BAL and serum (Fig. 2). In ALI, neutrophils are crucial for bacterial clearance during live infection, repair, and tissue remodeling after ALI (57, 58). Our data suggest that *lincRNA-Cox2* plays an important role in neutrophil recruitment and therefore could also play roles in clearance of live bacteria and repair of tissue after resolution of infection. We found that Il6 levels were reduced, while Ccl5 levels were increased, after ALI in the *lincRNA-Cox2* mutant mice. These findings are consistent with our previous in vitro and in vivo studies (28, 36). In addition, we found that Ccl3 and Ccl4 are positively regulated, while Ccl22 and Ifnb1 are negatively regulated, by *lincRNA-Cox2* in the lung during ALI. Interestingly, Lee et al. (59) and others (60–63) have reported that the chemokines, CCL3 and CCL4, promote the local influx of neutrophils. Therefore, the

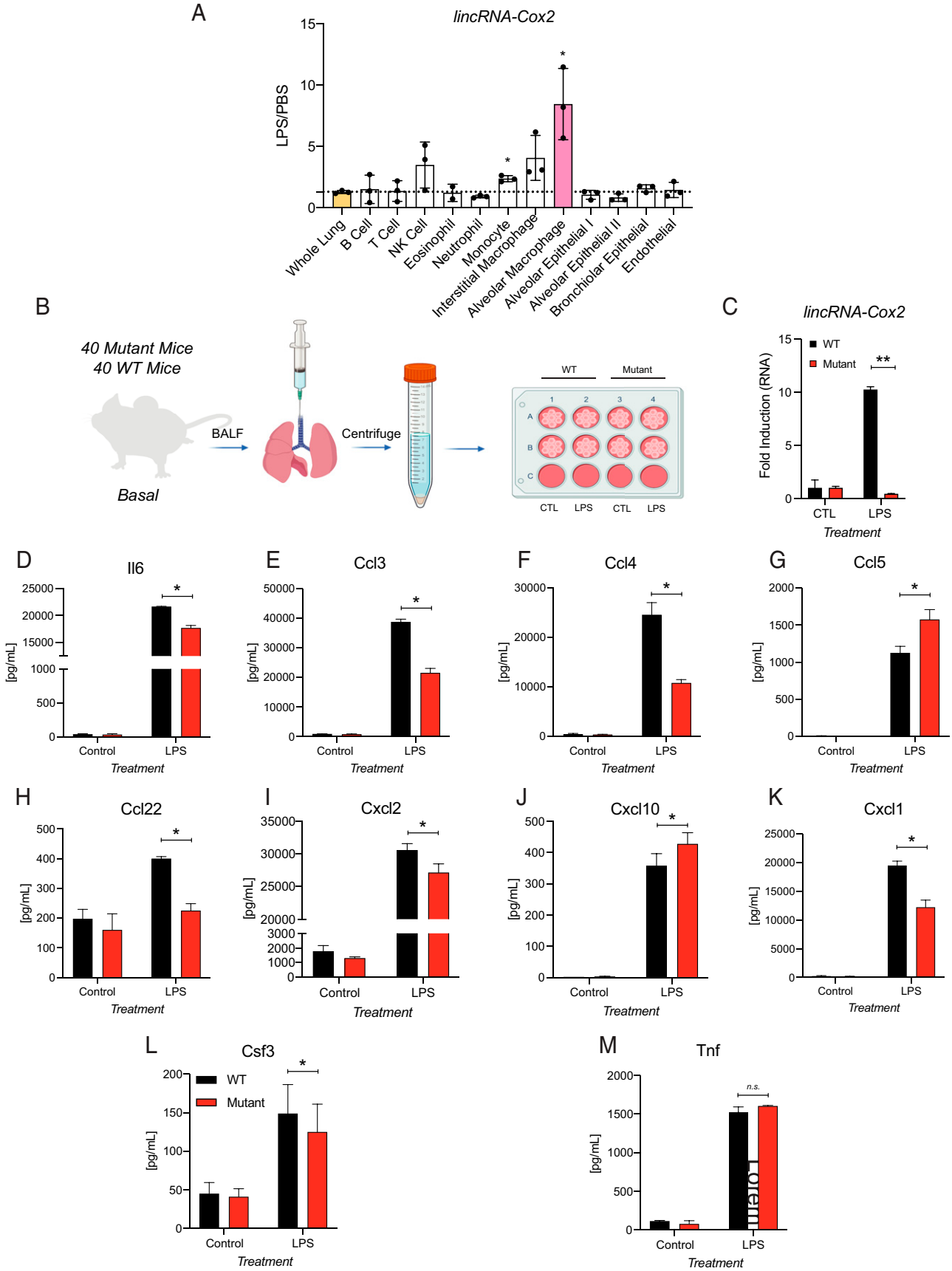

FIGURE 7. *lincRNA-Cox2* is inducible and regulates immune genes both positively and negatively in primary AMs. (**A**) *lincRNA-Cox2* was measured in whole-lung tissue and several sorted immune and epithelial cells from mice treated with PBS and LPS via an oropharyngeal route. Expression was normalized to PBS. Performed in biological triplicates, and Student *t* test was performed between whole-lung tissue and each sorted cell. (**B**) The experimental design is depicted. BALs harvested from 40 WT and 40 Mut mice and 10 WT or Mut mice were pooled per well. Cells were *(Figure legend continues)*

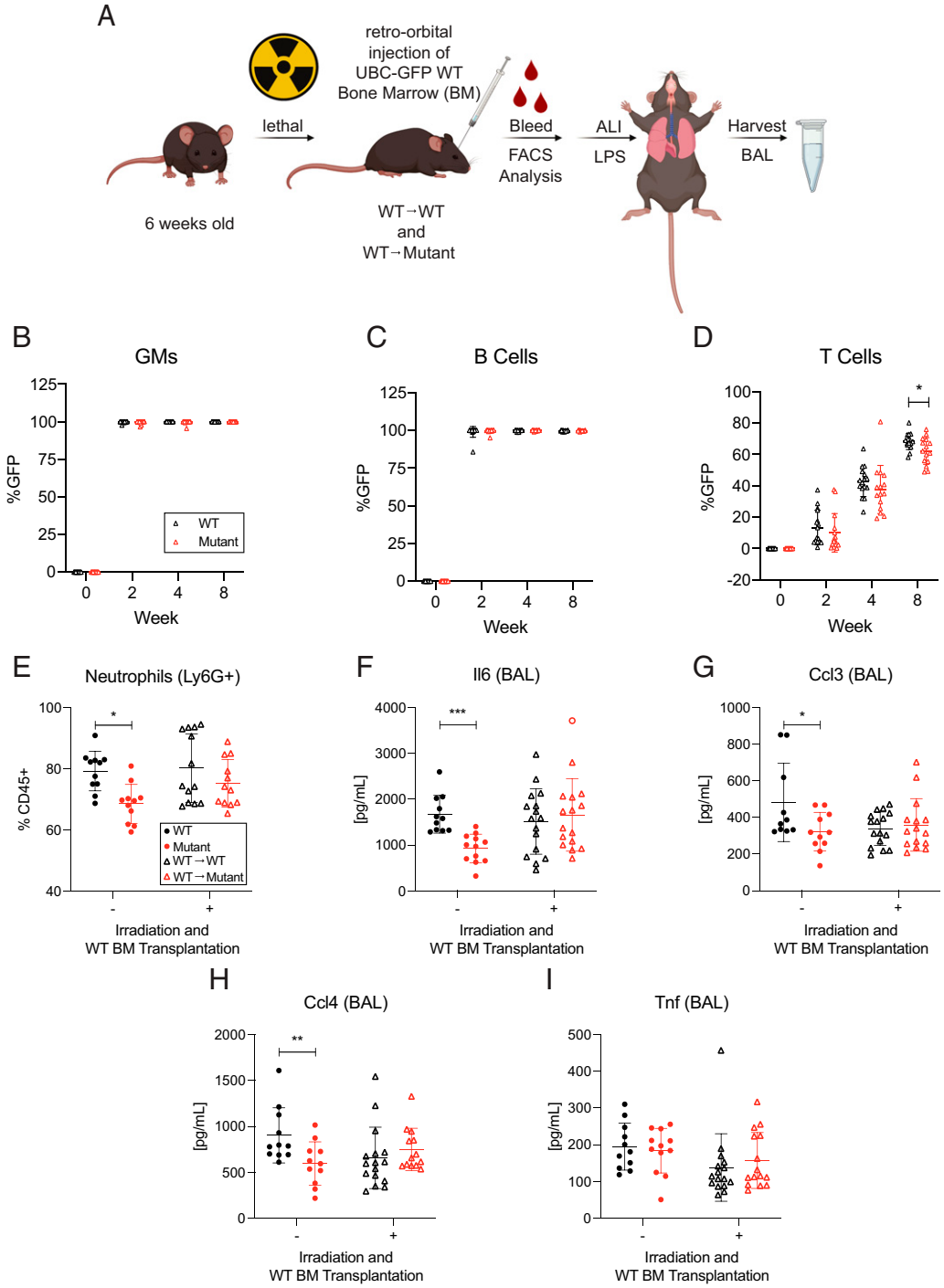

FIGURE 8. WT BM transplantation (BMT) in *lincRNA-Cox2* mutant mice rescues the ALI phenotype. (**A**) WT BMT and ALI experiment schematic. Chimerism was assessed in the PB by gating for GFP% of (**B**) GMs, (**C**) B cells, and (**D**) T cells. (**E**) Percentage of Ly6G$^+$ neutrophil populations were graphed for WT, Mut, WT→WT, and WT→Mut mice. Multiplex cytokine analysis was performed on BAL for (**F**) Il6, (**G**) Ccl3, (**H**) Ccl4, and (**I**) Tnf. Data of non-BMT mice experiments are from Figs. 2 and 5. Student *t* test was used to determine significance, and asterisks indicate statistical significance (*$p > 0.05$, **$p \geq 0.01$, ***$p > 0.0005$).

decreased expression of Ccl3 and Ccl4 in vivo in the *lincRNA-Cox2* mutant mice could explain the significant decrease of neutrophil recruitment seen in the BAL (Fig. 2B).

To date, there remains only a small number of lncRNAs that have been functionally and mechanistically characterized in vivo. In fact, Pnky, Tug1, and Firre are the only other lncRNA studies that show that their phenotype can be rescued in *trans* in vivo (64–66). From our previous in vivo studies, we had concluded that *lincRNA-Cox2* functions in *cis* to regulate Ptgs2 in an enhancer RNA manner, while it functions in *trans* to regulate genes such as Il6 and Ccl5 (36). To prove that indeed *lincRNA-Cox2* can function in *trans* to regulate immune genes, we generated a Tg mouse overexpressing *lincRNA-Cox2* from the H11 locus using the TARGATT system (37) (Fig. 3A, Supplemental Fig. 1). Simply overexpressing

treated with LPS for 24 h. (**C**) *lincRNA-Cox2* was measured by RT-qPCR in primary AMs. Multiplex cytokine analysis was performed for the supernatant from primary AMs for (**D**) Il6, (**E**) Ccl3, (**F**) Ccl4, (**G**) Ccl5, (**H**) Ccl22, (**I**) Cxcl2, (**J**) Cxcl10, (**K**) Cxcl1, (**L**) Csf3, (**M**) Tnf. Student *t* test used to determine significance, and asterisks indicate statistical significance (*$p > 0.05$, **$p \geq 0.01$).

lincRNA-Cox2 minimally impacts the immune response after an LPS septic shock model, but widely impacts genes using an LPS-induced ALI model, suggesting that *lincRNA-Cox2* is an important regulator of immune genes within the lung (Figs. 3, 4). Using the septic shock model, we do note that Csf1 and Il10 are lower in serum after endotoxic shock in the *lincRNA-Cox2* Tg mouse. However, in the ALI model, overexpression of *lincRNA-Cox2* resulted in an increase in Il6 and Ccl3 production within the BAL (Fig. 4), which is the opposite phenotype to that observed when *lincRNA-Cox2* is removed (Fig. 2). Unique to the overexpression of *lincRNA-Cox2* was the decreased levels of Timp1, and previous work indicates that dysregulation of Timp1 in the lungs is critical to resolution of lung injury, as well as evading live pathogen infection (38, 67–69). These data suggest that overexpression of *lincRNA-Cox2* in vivo could be in important model to study specific aspects of lung immune regulation.

Our primary goal for generating the Tg mouse line overexpressing *lincRNA-Cox2* was to determine whether crossing it to our *lincRNA-Cox2* mutant (deficient) mouse generating a MutxTG line (Fig. 5A) would rescue the phenotypes observed in the mutant line after LPS challenge using either an i.p. delivery or via oropharyngeal delivery. Interestingly, we found that our MutxTG mice do rescue the phenotype found in both the endotoxic shock model (Fig. 5) and LPS-induced ALI model (Fig. 6), showing definitively that *lincRNA-Cox2* regulates specific genes, as well as neutrophil recruitment in *trans*. Further work will need to be conducted to determine whether *lincRNA-Cox2* is functioning directly to regulate specific genes or whether it is indirect.

To delve more deeply into exactly how *lincRNA-Cox2* functions to regulate immune genes in the lung, we focused on determining in which cell type *lincRNA-Cox2* is most highly expressed. Analysis of scRNA-seq indicated that *lincRNA-Cox2* was highly expressed in naive and injured alveolar epithelial type II cells (Supplemental Fig. 5A–E); however, overall, *lincRNA-Cox2* was difficult to detect in single-cell data probably because of a combination of low expression levels and low read depth. Using FACS and qRT-PCR, we measured the expression of *lincRNA-Cox2* in eight immune cell populations and four epithelial/endothelial cell populations and found that *lincRNA-Cox2* was most highly expressed in neutrophils (Supplemental Fig. 5F, 5G). However, when assessing induction of *lincRNA-Cox2* after LPS and normalizing to PBS controls, we found it to be most highly expressed in AMs with some significant induction also observed in monocytes (Fig. 7A). We know AMs are critical effector cells in initiating and maintaining pulmonary inflammation, as well as termination and resolution of pulmonary inflammation during ALI (70, 71). Therefore, to determine whether the altered gene expression profiles we observed within the BAL after ALI were due to *lincRNA-Cox2* expression in AMs, we cultured primary AMs using previously published methods (43, 72, 73) from our WT and *lincRNA-Cox2* mutant mice and measured cytokine and chemokine expression. Excitingly, we found decreased expression of Il6, Ccl3, and Ccl4 and increased expression of Ccl5 in the *lincRNA-Cox2* mutant AMs (Fig. 7D–G), consistent with our in vivo findings from the BAL after ALI. Several other chemokines, such as Ccl3, Ccl4, Csf3, Cxcl1, and Cxcl2, were significantly lower in the *lincRNA-Cox2*–deficient AMs, and these all are known to play roles in neutrophil influx (59, 61, 74). These data suggest that *lincRNA-Cox2* functions within AMs to regulate gene expression, including key chemokines that can impact neutrophil infiltration during ALI.

During ALI, many of the immune cells that infiltrate the lung, including some classes of AMs, originate from the BM. Analysis of resident and recruited AMs during ALI showed *lincRNA-Cox2* is more highly expressed in recruited (BM-derived) AMs (Supplemental Fig. 6A, 6B). Therefore, to assess whether *lincRNA-Cox2* is functioning through BM-derived immune cells, we performed BM transplantation chimera experiments in WT and *lincRNA-Cox2* mutant mice (Fig. 7A). We found that WT→Mut BM transplantations completely rescued the neutrophil and cytokine/chemokine phenotype in the BAL (Fig. 8B–H, Supplemental Fig. 6L). Although we aimed to determine whether *lincRNA-Cox2* functions either through resident (SiglecF$^+$) or recruited (SiglecF$^-$) AMs, we found that both populations were composed of >70% donor BM (Supplemental Fig. 6J, 6K), indicating that radiation obliterated resident SiglecF$^+$ alveolar cells, which become repopulated with donor cells from the BM (51, 75–78). These experiments enabled us to conclude that *lincRNA-Cox2* expression originating from the BM can function to control immune responses in the lung, because BM-derived immune cells transplanted into *lincRNA-Cox2* mutant mice are able to rescue the phenotype driven by loss of *lincRNA-Cox2* in the lung. Although these data do rule out epithelial cells as a source of the *lincRNA-Cox2*–mediated phenotype, we did not examine any role for *lincRNA-Cox2* in other immune-infiltrating cells, such as neutrophils, and therefore cannot definitively rule them out as playing some role in addition to the AMs.

In conclusion, in this study, we show, through multiple mouse models, that *lincRNA-Cox2* is functioning in *trans* in AMs to regulate immune responses within the lung. This study provides an additional layer of mechanistic understanding highlighting that lncRNAs can contribute to the delicate balance between maintenance of homeostasis and induction of transient inflammation within the lung microenvironment.

Acknowledgments

We thank the UCSC Flow Cytometry Core Facility, RRID: SCR_021149, for technical assistance. In addition, we thank BioRender for creating a platform to easily generate figures using BioRender.com.

Disclosures

The authors have no financial conflicts of interest.

References

1. Moldoveanu, B., P. Otmishi, P. Jani, J. Walker, X. Sarmiento, J. Guardiola, M. Saad, and J. Yu. 2009. Inflammatory mechanisms in the lung. *J. Inflamm. Res.* 2: 1–11.
2. Mokra, D., and P. Kosutova. 2015. Biomarkers in acute lung injury. *Respir. Physiol. Neurobiol.* 209: 52–58.
3. Wang, Y.-C., Q.-X. Liu, Q. Zheng, T. Liu, X.-E. Xu, X.-H. Liu, W. Gao, X.-J. Bai, and Z.-F. Li. 2019. Dihydromyricetin alleviates sepsis-induced acute lung injury through inhibiting NLRP3 inflammasome-dependent pyroptosis in mice model. *Inflammation* 42: 1301–1310.
4. Mowery, N. T., W. T. H. Terzian, and A. C. Nelson. 2020. Acute lung injury. *Curr. Probl. Surg.* 57: 100777.
5. Butt, Y., A. Kurdowska, and T. C. Allen. 2016. Acute lung injury: a clinical and molecular review. *Arch. Pathol. Lab. Med.* 140: 345–350.
6. Pittet, J. F., R. C. Mackersie, T. R. Martin, and M. A. Matthay. 1997. Biological markers of acute lung injury: prognostic and pathogenetic significance. *Am. J. Respir. Crit. Care Med.* 155: 1187–1205.
7. Alluri, R., H. L. Kutscher, B. A. Mullan, B. A. Davidson, and P. R. Knight. 2017. Open tracheostomy gastric acid aspiration murine model of acute lung injury results in maximal acute nonlethal lung injury. *J. Vis. Exp.* 2017: 54700.
8. Gouda, M. M., and Y. P. Bhandary. 2019. Acute lung injury: IL-17A-mediated inflammatory pathway and its regulation by curcumin. *Inflammation* 42: 1160–1169.
9. Fan, E. K. Y., and J. Fan. 2018. Regulation of alveolar macrophage death in acute lung inflammation. *Respir. Res.* 19: 50.
10. Raghavendran, K., G. S. Pryhuber, P. R. Chess, B. A. Davidson, P. R. Knight, and R. H. Notter. 2008. Pharmacotherapy of acute lung injury and acute respiratory distress syndrome. *Curr. Med. Chem.* 15: 1911–1924.
11. Yin, J., and C.-X. Bai. 2018. Pharmacotherapy for adult patients with acute respiratory distress syndrome. *Chin. Med. J. (Engl.)* 131: 1138–1141.
12. Suo, T., G.-Z. Chen, Y. Huang, K.-C. Zhao, T. Wang, and K. Hu. 2018. miRNA-1246 suppresses acute lung injury-induced inflammation and apoptosis via the NF-κB and Wnt/β-catenin signal pathways. *Biomed. Pharmacother.* 108: 783–791.
13. Deng, G., H. He, Z. Chen, L. OuYang, X. Xiao, J. Ge, B. Xiang, S. Jiang, and S. Cheng. 2017. Lianqinjiedu decoction attenuates LPS-induced inflammation and

acute lung injury in rats via TLR4/NF-κB pathway. *Biomed. Pharmacother.* 96: 148–152.
14. Uszczynska-Ratajczak, B., J. Lagarde, A. Frankish, R. Guigó, and R. Johnson. 2018. Towards a complete map of the human long non-coding RNA transcriptome. *Nat. Rev. Genet.* 19: 535–548.
15. Fang, S., L. Zhang, J. Guo, Y. Niu, Y. Wu, H. Li, L. Zhao, X. Li, X. Teng, X. Sun, et al. 2018. NONCODEV5: a comprehensive annotation database for long non-coding RNAs. *Nucleic Acids Res.* 46(D1): D308–D314.
16. Robinson, E. K., S. Covarrubias, and S. Carpenter. 2020. The how and why of lncRNA function: an innate immune perspective. *Biochim. Biophys. Acta. Gene Regul. Mech.* 1863: 194419.
17. Statello, L., C.-J. Guo, L.-L. Chen, and M. Huarte. 2021. Gene regulation by long non-coding RNAs and its biological functions. [Published erratum appears in 2021 *Nat. Rev. Mol. Cell Biol.* 22: 159.] *Nat. Rev. Mol. Cell Biol.* 22: 96–118.
18. Quinn, J. J., and H. Y. Chang. 2016. Unique features of long non-coding RNA biogenesis and function. *Nat. Rev. Genet.* 17: 47–62.
19. Aftabi, Y., K. Ansarin, D. Shanehbandi, M. Khalili, E. Seyedrezazadeh, L. Rahbarnia, M. Asadi, A. Amiri-Sadeghan, V. Zafari, S. Eyvazi, et al. 2021. Long non-coding RNAs as potential biomarkers in the prognosis and diagnosis of lung cancer: a review and target analysis. *IUBMB Life* 73: 307–327.
20. Ma, T., H. Jia, P. Ji, Y. He, and L. Chen. 2021. Identification of the candidate lncRNA biomarkers for acute kidney injury: a systematic review and meta-analysis. *Expert Rev. Mol. Diagn.* 21: 77–89.
21. Viereck, J., and T. Thum. 2017. Circulating noncoding RNAs as biomarkers of cardiovascular disease and injury. *Circ. Res.* 120: 381–399.
22. Teng, X., J. Liao, L. Zhao, W. Dong, H. Xue, L. Bai, and S. Xu. 2021. Whole transcriptome analysis of the differential RNA profiles and associated competing endogenous RNA networks in LPS-induced acute lung injury (ALI). *PLoS One* 16: e0251359.
23. Wang, J., Y.-C. Shen, Z.-N. Chen, Z.-C. Yuan, H. Wang, D.-J. Li, K. Liu, and F.-Q. Wen. 2019. Microarray profiling of lung long non-coding RNAs and mRNAs in lipopolysaccharide-induced acute lung injury mouse model. *Biosci. Rep.* 39: BSR20181634.
24. Chen, C., Y. He, Y. Feng, W. Hong, G. Luo, and Z. Ye. 2021. Long non-coding RNA review and implications in acute lung inflammation. *Life Sci.* 269: 119044.
25. Asti, C., V. Ruggieri, S. Porzio, R. Chiusaroli, G. Melillo, and G. F. Caselli. 2000. Lipopolysaccharide-induced lung injury in mice. I. Concomitant evaluation of inflammatory cells and haemorrhagic lung damage. *Pulm. Pharmacol. Ther.* 13: 61–69.
26. Dai, L., G. Zhang, Z. Cheng, X. Wang, L. Jia, X. Jing, H. Wang, R. Zhang, M. Liu, T. Jiang, et al. 2018. Knockdown of LncRNA MALAT1 contributes to the suppression of inflammatory responses by up-regulating miR-146a in LPS-induced acute lung injury. *Connect. Tissue Res.* 59: 581–592.
27. Li, J., L. Xue, Y. Wu, Q. Yang, D. Liu, C. Yu, and J. Peng. 2021. STAT3-activated lncRNA XIST accelerates the inflammatory response and apoptosis of LPS-induced acute lung injury. *J. Cell. Mol. Med.* 25: 6550–6557.
28. Carpenter, S., D. Aiello, M. K. Atianand, E. P. Ricci, P. Gandhi, L. L. Hall, M. Byron, B. Monks, M. Henry-Bezy, J. B. Lawrence, et al. 2013. A long noncoding RNA mediates both activation and repression of immune response genes. *Science* 341: 789–792.
29. Tong, Q., A.-Y. Gong, X.-T. Zhang, C. Lin, S. Ma, J. Chen, G. Hu, and X.-M. Chen. 2016. LincRNA-Cox2 modulates TNF-α-induced transcription of Il12b gene in intestinal epithelial cells through regulation of Mi-2/NuRD-mediated epigenetic histone modifications. *FASEB J.* 30: 1187–1197.
30. Hu, G., A.-Y. Gong, Y. Wang, S. Ma, X. Chen, J. Chen, C.-J. Su, A. Shibata, J. K. Strauss-Soukup, K. M. Drescher, and X.-M. Chen. 2016. LincRNA-Cox2 promotes late inflammatory gene transcription in macrophages through modulating SWI/SNF-mediated chromatin remodeling. *J. Immunol.* 196: 2799–2808.
31. Covarrubias, S., E. K. Robinson, B. Shapleigh, A. Vollmers, S. Katzman, N. Hanley, N. Fong, M. T. McManus, and S. Carpenter. 2017. CRISPR/Cas-based screening of long non-coding RNAs (lncRNAs) in macrophages with an NF-κB reporter. *J. Biol. Chem.* 292: 20911–20920.
32. Hu, G., K. Liao, F. Niu, L. Yang, B. W. Dallon, S. Callen, C. Tian, J. Shu, J. Cui, Z. Sun, et al. 2018. Astrocyte EV-induced lincRNA-Cox2 regulates microglial phagocytosis: implications for morphine-mediated neurodegeneration. *Mol. Ther. Nucleic Acids* 13: 450–463.
33. Liao, K., F. Niu, R. S. Dagur, M. He, C. Tian, and G. Hu. 2020. Intranasal delivery of lincRNA-Cox2 siRNA loaded extracellular vesicles decreases lipopolysaccharide-induced microglial proliferation in mice. *J. Neuroimmune Pharmacol.* 15: 390–399.
34. Xue, Z., Z. Zhang, H. Liu, W. Li, X. Guo, Z. Zhang, Y. Liu, L. Jia, Y. Li, Y. Ren, et al. 2019. lincRNA-Cox2 regulates NLRP3 inflammasome and autophagy mediated neuroinflammation. *Cell Death Differ.* 26: 130–145.
35. Sauvageau, M., L. A. Goff, S. Lodato, B. Bonev, A. F. Groff, C. Gerhardinger, D. B. Sanchez-Gomez, E. Hacisuleyman, E. Li, M. Spence, et al. 2013. Multiple knockout mouse models reveal lincRNAs are required for life and brain development. *eLife* 2: e01749.
36. Elling, R., E. K. Robinson, B. Shapleigh, S. C. Liapis, S. Covarrubias, S. Katzman, A. F. Groff, Z. Jiang, S. Agarwal, M. Motwani, et al. 2018. Genetic models reveal cis and trans immune-regulatory activities for lincRNA-Cox2. *Cell Rep.* 25: 1511–1524.e6.
37. Tasic, B., S. Hippenmeyer, C. Wang, M. Gamboa, H. Zong, Y. Chen-Tsai, and L. Luo. 2011. Site-specific integrase-mediated transgenesis in mice via pronuclear injection. *Proc. Natl. Acad. Sci. USA* 108: 7902–7907.
38. Allen, I. C. 2014. The utilization of oropharyngeal intratracheal PAMP administration and bronchoalveolar lavage to evaluate the host immune response in mice. *J. Vis. Exp.* 2014: 51391 .
39. Nielsen, T. B., J. Yan, B. Luna, and B. Spellberg. 2018. Murine oropharyngeal aspiration model of ventilator-associated and hospital-acquired bacterial pneumonia. *J. Vis. Exp.* 2018: 57672.
40. Ehrentraut, H., C. K. Weisheit, S. Frede, and T. Hilbert. 2019. Inducing acute lung injury in mice by direct intratracheal lipopolysaccharide instillation. *J. Vis. Exp.* 2019: e59999.
41. Poscablo, D. M., A. K. Worthington, S. Smith-Berdan, and E. C. Forsberg. 2021. Megakaryocyte progenitor cell function is enhanced upon aging despite the functional decline of aged hematopoietic stem cells. *Stem Cell Reports* 16: 1598–1613.
42. Cloonan, S. M., K. Glass, M. E. Laucho-Contreras, A. R. Bhashyam, M. Cervo, M. A. Pabón, C. Konrad, F. Polverino, I. I. Siempos, E. Perez, et al. 2016. Mitochondrial iron chelation ameliorates cigarette smoke-induced bronchitis and emphysema in mice. *Nat. Med.* 22: 163–174.
43. Robinson, E. K., S. Covarrubias, S. Zhou, and S. Carpenter. 2021. Generation and utilization of a HEK-293T murine GM-CSF expressing cell line. *PLoS One* 16: e0249117.
44. Chen, B. D., M. Mueller, and T. H. Chou. 1988. Role of granulocyte/macrophage colony-stimulating factor in the regulation of murine alveolar macrophage proliferation and differentiation. *J. Immunol.* 141: 139–144.
45. Yu, Y.-R. A., E. G. O'Koren, D. F. Hotten, M. J. Kan, D. Kopin, E. R. Nelson, L. Que, and M. D. Gunn. 2016. A protocol for the comprehensive flow cytometric analysis of immune cells in normal and inflamed murine non-lymphoid tissues. *PLoS One* 11: e0150606.
46. Nakano, H., K. Nakano, and D. N. Cook. 2018. Isolation and purification of epithelial and endothelial cells from mouse lung. *Methods Mol. Biol.* 1799: 59–69.
47. Mould, K. J., L. Barthel, M. P. Mohning, S. M. Thomas, A. L. McCubbrey, T. Danhorn, S. M. Leach, T. E. Fingerlin, B. P. O'Connor, J. A. Reisz, et al. 2017. Cell origin dictates programming of resident versus recruited macrophages during acute lung injury. *Am. J. Respir. Cell Mol. Biol.* 57: 294–306.
48. Mould, K. J., N. D. Jackson, P. M. Henson, M. Seibold, and W. J. Janssen. 2019. Single cell RNA sequencing identifies unique inflammatory airspace macrophage subsets. *JCI Insight* 4: e126556.
49. Riemondy, K. A., N. L. Jansing, P. Jiang, E. F. Redente, A. E. Gillen, R. Fu, A. J. Miller, J. R. Spence, A. N. Gerber, J. R. Hesselberth, and R. L. Zemans. 2019. Single cell RNA sequencing identifies TGFβ as a key regenerative cue following LPS-induced lung injury. *JCI Insight* 5: e123637.
50. Wolf, F. A., P. Angerer, and F. J. Theis. 2018. SCANPY: large-scale single-cell gene expression data analysis. *Genome Biol.* 19: 15.
51. Hashimoto, D., A. Chow, C. Noizat, P. Teo, M. B. Beasley, M. Leboeuf, C. D. Becker, P. See, J. Price, D. Lucas, et al. 2013. Tissue-resident macrophages self-maintain locally throughout adult life with minimal contribution from circulating monocytes. *Immunity* 38: 792–804.
52. Domscheit, H., M. A. Hegeman, N. Carvalho, and P. M. Spieth. 2020. Molecular dynamics of lipopolysaccharide-induced lung injury in rodents. *Front. Physiol.* 11: 36.
53. Ali, H., A. Khan, J. Ali, H. Ullah, A. Khan, H. Ali, N. Irshad, and S. Khan. 2020. Attenuation of LPS-induced acute lung injury by continentalic acid in rodents through inhibition of inflammatory mediators correlates with increased Nrf2 protein expression. *BMC Pharmacol. Toxicol.* 21: 81.
54. Menon, M., T. Hussell, and H. Ali Shuwa. 2021. Regulatory B cells in respiratory health and diseases. *Immunol. Rev.* 299: 61–73.
55. Seys, L. J. M., F. M. Verhamme, A. Schinwald, H. Hammad, D. M. Cunoosamy, C. Bantsimba-Malanda, A. Sabirsh, E. McCall, L. Flavell, R. Herbst, et al. 2015. Role of B Cell-Activating Factor in Chronic Obstructive Pulmonary Disease. *Am. J. Respir. Crit. Care Med.* 192: 706–718.
56. Cook, P. C., and A. S. MacDonald. 2016. Dendritic cells in lung immunopathology. *Semin. Immunopathol.* 38: 449–460.
57. Blázquez-Prieto, J., I. López-Alonso, C. Huidobro, and G. M. Albaiceta. 2018. The emerging role of neutrophils in repair after acute lung injury. *Am. J. Respir. Cell Mol. Biol.* 59: 289–294.
58. Giacalone, V. D., C. Margaroli, M. A. Mall, and R. Tirouvanziam. 2020. Neutrophil adaptations upon recruitment to the lung: new concepts and implications for homeostasis and disease. *Int. J. Mol. Sci.* 21: 851.
59. Lee, S. C., M. E. Brummet, S. Shahabuddin, T. G. Woodworth, S. N. Georas, K. M. Leiferman, S. C. Gilman, C. Stellato, R. P. Gladue, R. P. Schleimer, and L. A. Beck. 2000. Cutaneous injection of human subjects with macrophage inflammatory protein-1 alpha induces significant recruitment of neutrophils and monocytes. *J. Immunol.* 164: 3392–3401.
60. Rudd, J. M., S. Pulavendran, H. K. Ashar, J. W. Ritchey, T. A. Snider, J. R. Malayer, M. Marie, V. T. K. Chow, and T. Narasaraju. 2019. Neutrophils induce a novel chemokine receptors repertoire during influenza pneumonia. *Front. Cell. Infect. Microbiol.* 9: 108.
61. Metzemaekers, M., M. Gouwy, and P. Proost. 2020. Neutrophil chemoattractant receptors in health and disease: double-edged swords. *Cell. Mol. Immunol.* 17: 433–450.
62. Ramos, C. D. L., C. Canetti, J. T. Souto, J. S. Silva, C. M. Hogaboam, S. H. Ferreira, and F. Q. Cunha. 2005. MIP-1alpha[CCL3] acting on the CCR1 receptor mediates neutrophil migration in immune inflammation via sequential release of TNF-alpha and LTB4. *J. Leukoc. Biol.* 78: 167–177.
63. Bonville, C. A., C. M. Percopo, K. D. Dyer, J. Gao, C. Prussin, B. Foster, H. F. Rosenberg, and J. B. Domachowske. 2009. Interferon-gamma coordinates CCL3-mediated neutrophil recruitment in vivo. *BMC Immunol.* 10: 14.
64. Andersen, R. E., S. J. Hong, J. J. Lim, M. Cui, B. A. Harpur, E. Hwang, R. N. Delgado, A. D. Ramos, S. J. Liu, B. J. Blencowe, and D. A. Lim. 2019. The long noncoding RNA Pnky is a trans-acting regulator of cortical development in vivo. *Dev. Cell* 49: 632–642.e7.

65. Lewandowski, J. P., J. C. Lee, T. Hwang, H. Sunwoo, J. M. Goldstein, A. F. Groff, N. P. Chang, W. Mallard, A. Williams, J. Henao-Meija, et al. 2019. The Firre locus produces a trans-acting RNA molecule that functions in hematopoiesis. *Nat. Commun.* 10: 5137.
66. Lewandowski, J. P., G. Dumbović, A. R. Watson, T. Hwang, E. Jacobs-Palmer, N. Chang, C. Much, K. M. Turner, C. Kirby, N. D. Rubinstein, et al. 2020. The Tug1 lncRNA locus is essential for male fertility. *Genome Biol.* 21: 237.
67. Nolan, A., S. Kwon, S. J. Cho, B. Naveed, A. L. Comfort, D. J. Prezant, W. N. Rom, and M. D. Weiden. 2014. MMP-2 and TIMP-1 predict healing of WTC-lung injury in New York City firefighters. *Respir. Res.* 15: 5.
68. Chen, G., D. Ge, B. Zhu, H. Shi, and Q. Ma. 2020. Upregulation of matrix metalloproteinase 9 (MMP9)/tissue inhibitor of metalloproteinase 1 (TIMP1) and MMP2/TIMP2 ratios may be involved in lipopolysaccharide-induced acute lung injury. *J. Int. Med. Res.* 48: 300060520919592.
69. Davey, A., D. F. McAuley, and C. M. O'Kane. 2011. Matrix metalloproteinases in acute lung injury: mediators of injury and drivers of repair. *Eur. Respir. J.* 38: 959–970.
70. Beck-Schimmer, B., R. Schwendener, T. Pasch, L. Reyes, C. Booy, and R. C. Schimmer. 2005. Alveolar macrophages regulate neutrophil recruitment in endotoxin-induced lung injury. *Respir. Res.* 6: 61.
71. Herold, S., K. Mayer, and J. Lohmeyer. 2011. Acute lung injury: how macrophages orchestrate resolution of inflammation and tissue repair. *Front. Immunol.* 2: 65.
72. Machiels, B., M. Dourcy, X. Xiao, J. Javaux, C. Mesnil, C. Sabatel, D. Desmecht, F. Lallemand, P. Martinive, H. Hammad, et al. 2017. A gammaherpesvirus provides protection against allergic asthma by inducing the replacement of resident alveolar macrophages with regulatory monocytes. [Published erratum appears in 2018 *Nat. Immunol.* 19: 1035.] *Nat. Immunol.* 18: 1310–1320.
73. Nayak, D. K., O. Mendez, S. Bowen, and T. Mohanakumar. 2018. Isolation and in vitro culture of murine and human alveolar macrophages. *J. Vis. Exp.* 2018: 57287.
74. Kobayashi, Y. 2008. The role of chemokines in neutrophil biology. *Front. Biosci.* 13: 2400–2407.
75. Guilliams, M., I. De Kleer, S. Henri, S. Post, L. Vanhoutte, S. De Prijck, K. Deswarte, B. Malissen, H. Hammad, and B. N. Lambrecht. 2013. Alveolar macrophages develop from fetal monocytes that differentiate into long-lived cells in the first week of life via GM-CSF. *J. Exp. Med.* 210: 1977–1992.
76. Misharin, A. V., L. Morales-Nebreda, P. A. Reyfman, C. M. Cuda, J. M. Walter, A. C. McQuattie-Pimentel, C.-I. Chen, K. R. Anekalla, N. Joshi, K. J. N. Williams, et al. 2017. Monocyte-derived alveolar macrophages drive lung fibrosis and persist in the lung over the life span. *J. Exp. Med.* 214: 2387–2404.
77. Collins, M. K., A. M. Shotland, M. F. Wade, S. M. Atif, D. K. Richards, M. Torres-Llompart, D. G. Mack, A. K. Martin, A. P. Fontenot, and A. S. McKee. 2020. A role for TNF-α in alveolar macrophage damage-associated molecular pattern release. *JCI Insight* 5: e134356.
78. Gangwar, R. S., V. Vinayachandran, P. Rengasamy, R. Chan, B. Park, R. Diamond-Zaluski, E. A. Cara, A. Cha, L. Das, C. Asase, et al. 2020. Differential contribution of bone marrow-derived infiltrating monocytes and resident macrophages to persistent lung inflammation in chronic air pollution exposure. *Sci. Rep.* 10: 14348.